PB-237 808-T

PARTICLE SIZE MEASUREMENT BY PHOTOMULTIPLIER

Katsuya Oki, et al

Environmental Protection Agency
Research Triangle Park, North Carolina

September 1974

DISTRIBUTED BY:

NTIS

National Technical Information Service
U. S. DEPARTMENT OF COMMERCE

312038

NTIS

PB 237 808-T

EPA-TR 35-75

PARTICLE SIZE MEASUREMENT BY PHOTOMULTIPLIER
[Kōdenshi zōbaikan ni yoru ryūshikei no sokutei]

by

Katsuya Ōki, Takashi Akehata, and Takashi Shirai
Tokyo Institute of Technology, Resources Chemistry Research Institute

Published in Funtai Kōgaku Kenkyūkai-shi
[Journal of the Research Association of Powder Technology, Japan]
Vol. 10, No. 4, May 1973, pp. 195-203.

A novel, convenient method of particle size measurement by use of a photomultiplier is proposed. The measuring equipment consisted of a source of parallel light beams and an optical fiber connected to a photomultiplier which was used as a detector for the variation of light intensity. When one particle passed through the detecting section, the output of the photomultiplier changed according to the diameter of the particle. The relationship between the photomultiplier output and the particle diameter was numerically computed by using the theory of geometrical optics, and the results were confirmed experimentally. This report describes the computed results, the circuit for measurement, the method of calibrating the detectors, the estimation of errors due to the coexistence of particles in the slit, and examples of particle size measurements. By applying this method, particle size distribution could easily be determined with a very small amount of samples in a much shorter time than any other method ever used.

Translated for Tech. Publications Branch, Information Services Division, EPA, by LEO KANNER ASSOCIATES, P.O. Box 5187, Redwood City, California 94063, (415) 365-3046, September 1974.

Reproduced by
NATIONAL TECHNICAL
INFORMATION SERVICE
U S Department of Commerce
Springfield VA 22151

Q

28

Introduction

There exist numerous methods for measuring particle size distributions [1, 2]. Measuring devices sold on the market and suitable for various particle sizes have been in wide use in the past for particles ranging in size from about 10^{-6} mm up to several mm, and books concerning them have also been published. For example, sieves are ordinarily used for differentiating particles of more than 40 microns. However, there are considerable problems in actual practice, such as the precision of the sieve apertures, the question of clogging of the apertures, and the length of the sifting time. Furthermore, there is a poor efficiency, since much labor is required to measure one by one the weights of the samples after sieve analysis. Another inconvenience is the fact that the method can be used only for dry solid particles.

The writers developed equipment using photomultipliers for measuring particle sizes simply and accurately using a small amount of samples, which may be either solid or liquid particles. Since good results were obtained, they are reported here. The report deals with the basic principles of the optical method utilized in the measurements, the related calculations based on geometrical optics, the methods of calibrating the equipment, and the processing of the electrical signals obtained from the equipment.

1. Basic Principles of Measurement

1.1. Principles

In Fig. 1, when particles enter the space between the pencil of parallel light beams P passing in through the slit from the left side and the light receiver, which has a definite area, since part of the light will undergo reflection or absorption by the particles, there will be a reduction of the intensity of illumination of the light receiver. The degree of reduction will be determined both by the optical properties of the particles and by the particle size. If one uses a photomultiplier to convert the reduction of the intensity of illumination of the light receiver into voltage and to record it, it will be possible to find, by means of the voltage peak values, the diameters of each of the particles passing one by one through the measuring part shown in Fig. 1.

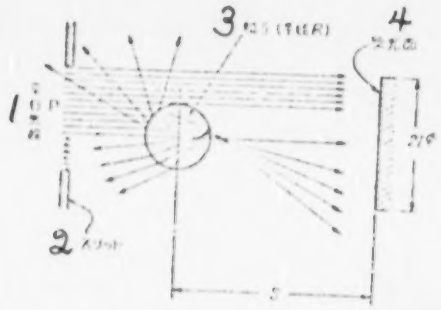

Fig. 1. Explanatory diagram of basic principles of measurement

Key:
1. Parallel light beams
2. Slit
3. Particle (radius R)
4. Light receiver

1.2. Relationship between Particle Size and Changes in Intensity of Illumination on Light Receiver

The decrease in the intensity of illumination ΔF on the light receiver (surface area A_R) when particles are present is given by the following:

$$\Delta F = \pi R^2 I_0 k / A_R \tag{1}$$

Here, R is the particle radius, I_0 is the parallel light beam pencil passing through a unit of area, and k is the ratio of the incident parallel light beam pencil which reaches the particle surface but does not reach the light receiver. If the value of k is known, one can find the relationship between the particle size and the decrease in the intensity of illumination on the light receiver. Since this k value depends on the optical properties of the particles, the distance S between the particle and the light receiver, and the area of the light receiver A_R, one first seeks the relationships between them by calculation. In this case, we assumed that the particle sizes were sufficiently greater than the wavelengths of the light. For the sake of simplicity, we assumed that the shapes were spherical, and calculations were performed by the methods of geometrical optics [3] for two cases: first, when the particles were transparent particles with zero absorption of light; and second, when the particles had perfectly mirror surfaces.

1.3. Calculation of k

As is shown in Fig. 2, a single light ray P is used to represent the path of the uniform luminous flux which enters from the right side, passes parallel to the Y axis through a finite, hypothetical area element $r_j \Delta r \Delta\theta$, and is admitted to the particle.

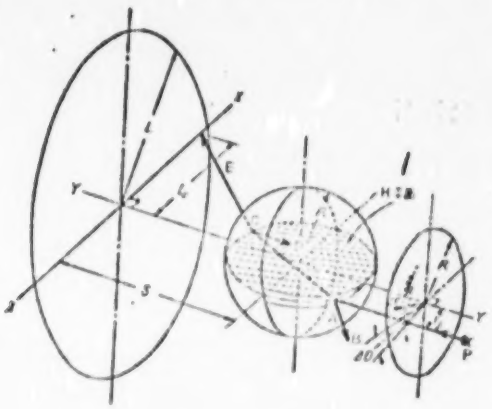

Reproduced from best available copy.

Fig. 2. Explanatory diagram of the path of the light rays incident to the particle

Key: 1. H plane

Part of the light ray admitted to point A on the particle surface is reflected towards direction B on the H plane, which is shown by the slanted lines in the figure. The remainder passes through the inside of the particle and reaches point C. Another part of it is reflected towards direction D and repeats similar reflection and refraction. On the other hand, the light refracted at point C and headed towards direction E outside of the particle reaches a point at a distance l_x on

axis x on the light receiver, which is removed from the particle by a distance of S. The H plane in Fig. 2 is redrawn in Fig. 3 with reference to the path of the light and the angular relationships involved. In this figure, the light ray P enters from above and is admitted to point A at a distance r_j away from the Y axis. If the refractive index is n, the angle of incidence ϕ_1 of the incident light ray P and its angle of reflection ϕ_0 will be, respectively:

$$\phi_1 = \tan^{-1}(r_j/\sqrt{R^2 - r_j^2}) \tag{2}$$

$$\phi_0 = \tan^{-1}(r_j/\sqrt{R^2 n^2 - r_j^2}) \tag{3}$$

When the incident light passes through the boundary between the particle and the medium on the i-th time ($i \geq 2$), the incident angle and the angle of refraction will each be geometrically the reverse of ϕ_0 and ϕ_1.

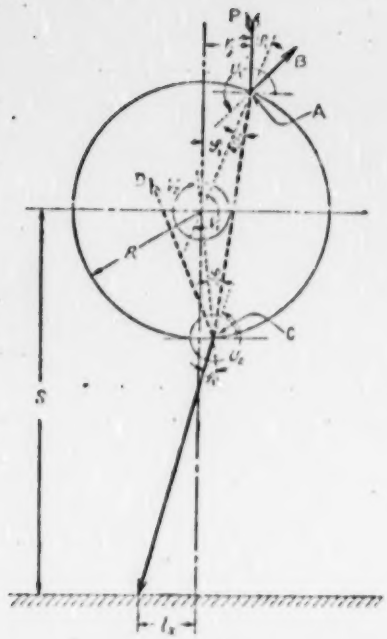

Fig. 3. Explanatory diagram of the path of the light ray on the H plane (Fig. 2)

On the other hand, the position coordinates and direction of the light ray departing from the particle can be found in the following manner by using angles U_i and V_i indicated in Fig. 3. First of all, U_i and V_i will be as follows, if we use the ϕ_1 and ϕ_0 of equations (2) and (3):

$$U_i = 2i\varphi_0 - \varphi_1 + (\pi/2 - \varphi_1) + (i+1)\pi \tag{4}$$

$$V_i = \varphi_1 + i(\pi - 2\varphi_0) + \pi \tag{5}$$

Consequently, l_x will be as follows, on account of equations (4) and (5):

$$l_x = -(S - R\cos V_i)\cdot\cot U_i - R\sin V_i \tag{6}$$

Since the intensity of the light ray incident at position r_j from axis Y will be proportional to the light flux incident at area element $r_i \Delta r \Delta\theta$, it can be expressed as ρ_j in the following terms:

$$\rho_j = \rho_1 \times (2j-1) \tag{7}$$

Here, ρ_1 expresses the intensity of the light passing through area element $(\Delta r)^2 \cdot \Delta\theta/2$. Consequently, if we use μ for the reflectance of the particle, after the light ray has been admitted at an intensity of ρ_j into the position r_j away from the axis Y, it will undergo repeated reflections inside the particle for i times. The intensity of the light as it goes outside of the particle, I_j, will be as follows if we consider the fact that its intensity will be attenuated by μ times at each reflection:

$$I_j = \rho_j \times (1-\mu)^2 \times \mu^{i-1} \tag{8}$$

Here, μ is given by Fresnel's equation [4]:

$$\mu = \frac{1}{2}\left\{ \frac{\sin^2(\varphi_1 - \varphi_0)}{\sin^2(\varphi_1 + \varphi_0)} + \frac{\tan^2(\varphi_1 - \varphi_0)}{\tan^2(\varphi_1 + \varphi_0)} \right\} \tag{9}$$

Let us vary the incident positions of the incident light, r_j(= $\Delta r/2$ + $\Delta r(j-1)$, Δr = R/N) and calculate one after another, using a digital computer, the coordinates l_x and the intensities I_j of each of the light rays when they have reached the X coordinate on the light receiver. In the calculations we use equations (6) and (8). Then let us use I to represent the integrated value of the intensity of the light rays after they have gone inside the light receiver ($|l_x| \leqq L$).

In this case, the following can be used to calculate the ratio k of the luminous flux departing outside of the light receiver with respect to the luminous flux admitted into the circular section of the particle:

$$k = \frac{\text{(Incident light flux)} - \text{(Light flux which has entered the light receiver)}}{\text{(Incident light flux)}}$$

$$= 1 - \frac{I}{\sum_j p_j} \qquad (10)$$

The relationships between the value k calculated in this manner and the distance S between the light receiver and the particle center are shown in Figs. 4-a and 4-b for transparent particles and particles with perfect mirror surfaces, respectively. There is a greater k value when S is great and the light receiver area A_R is small. It is clear that most of the incident luminous flux departs outside of the light receiver. Particles with perfect mirror surfaces, naturally enough, have a larger k value than transparent particles under the identical conditions.

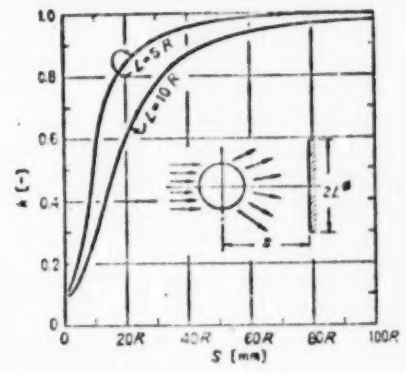

Fig. 4-a. Influence of L and S on coefficient k in equation (1). (For transparent spherical particles, calculated with n = 1.5)

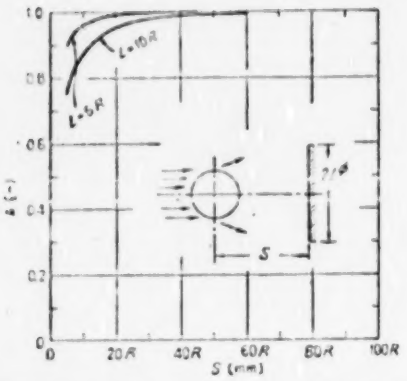

Fig. 4-b. Influence of L and S on coefficient k in equation (1). (For spherical particles with perfect mirror surfaces)

Furthermore, after the parallel light rays which have entered the circular section of the particle ($|r_j| < R$) have undergone reflection and refraction on account of the presence of the particle, they will display a localized intensity distribution of the light focused on the X axis on the light receiver as shown in Fig. 5. This light intensity distribution was found by segmenting the x axis into equally spaced microintervals Δx and integrating the intensity of the light rays reaching each of these intervals. It is clear from the figure that when S = 5R, the incident light ray pencil will be concentrated in the vicinity of the center of the light receiver, but that it will be widely dispersed as the S is increased.

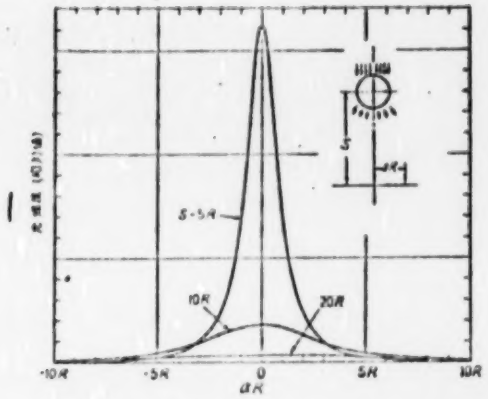

Fig. 5. Light intensity distribution on x axis on light receiver (calculated under the assumption that n = 1.5)

In carrying out the calculations to find k from equation (10), the numbers of the parallel incident light rays were varied. It was found that variations in the values of k would almost cease when the number of rays exceeded 5,000, so that the values would converge at a constant value. Therefore, in the subsequent calculations, we proceeded on the assumption that the number of incident light rays was 5,000. For the same reasons, the maximum number of reflections of the light rays inside the particles was set at i = 10 times.

1.4. Relationship between Photomultiplier Voltage Output and Particle Size

Let us use V_0 for the photomultiplier output corresponding to F_0, the intensity of illumination on the light receiver when particles are not present, and ΔV for the output decrease when the intensity of illumination has decreased by ΔF on account of the presence of the particles. In

this case, a proportional relationship of $V \propto F$ will apply between the intensity of illumination F and the photomultiplier output V. Therefore, the following relationship can be sought from equation (1).

$$\frac{\Delta F}{F} = \frac{\Delta V}{V_0} = \frac{\pi R^2 I_0}{A_s I_0} \cdot k = \frac{\pi R^2}{A_s} \cdot k \tag{11}$$

Here it is assumed that the area of the light receiver A_R remains constant. Furthermore, if the conditions are selected so that the physical properties of the particles will be identical, as was described in section 1.2, and so that the distance between the particles and the light receiver will be $k \approx 1$, as was shown in Fig. 4, the following proportional relationship will apply, on the basis of equation (11), between the particle size d_p (= 2R) and the square root of the voltage decrement ΔV:

$$d_p = \frac{2\sqrt{A_R}}{\sqrt{\pi k}} \sqrt{\frac{\Delta V}{V_0}} = C\sqrt{\frac{\Delta V}{V_0}} \tag{12}$$

Consequently, if we make F_0, that is, the output of the photomultiplier V_0, constant by making the light source output constant, and measure the output variations ΔV for the individual particles, we will be able to use equation (12) to find the particle diameter d_p. In the case of non-spherical particles, the equivalent diameter of the projected area circle will be sought.

2. Measuring Equipment and Methods of Processing the Detected Signals

2.1. Measuring Equipment

The particle size measuring unit is shown in outline in Fig. 6. The light coming from the 2.5V tungsten lamp a passes through the pinhole b and becomes parallel light beams in the lens c. Passing through the slit of the particle passage d, it enters the glass fiber light receiver. The other end of the glass fiber is connected to the light receiving part of the 1P21 photomultiplier. A linear relationship exists over a broad range between the light input of the photomultiplier and the output [5]. A high-voltage stabilized power source (model HD, 1.0 KM) manufactured by Ikegami Tsushinki Sha was used as the voltage source for supply to the anode. The slit d of the particle passage is of a rectangular shape and is made by stacking up glass plates. Two types of slits were used. They had different areas: 2×2 mm^2 (I) and 0.5×0.5 mm^2 (II). As for the distance S between the particle passage and the light receiver, it was made S = 30 mm so that $k \approx 1$.

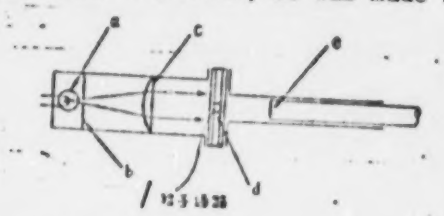

Fig. 6. Outline diagram of the measuring unit (when the particle passage was viewed from above)

Key:
a: Tungsten lamp
b: Pinhole
c: Lens
d: Slit
e: Bundle of optical fiber for receiving light
1. Particle passage

2.2. Methods of Processing the Signals

Electromagnetic oscillograph method. In Fig. 7 is shown an example of the photomultiplier output which has been amplified and recorded with an electromagnetic oscillograph (Vidigraph, manufactured by San'ei Sokki). Since the altitudes of these pulses are directly proportional to the output voltage, direct readings can be taken of these altitudes with a ruler. The ratio of the V_0 to the altitude is then sought, and the particle size can then be sought from equation (12).

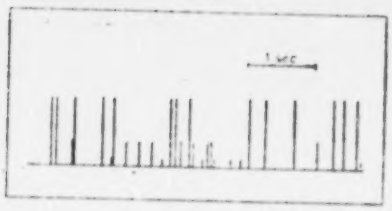

Fig. 7. An example of an electromagnetic oscillogram of the detected pulses. (1.589 mm spherical glass particles and 0.6 mm and 1.0 mm spherical steel particles)

Data recorder-comparator method. The aforementioned method of processing the signals requires the time and labor of reading the pulse heights with a ruler. Thus, it was decided to give the signals analog processing and to use also a digital counter. In order to shorten the signal processing time, the output signals were recorded once in a data recorder (TEAC, R-200). Then a comparator (voltage comparator, Mitsubishi

Electrical Corporation IC, M51710T) was used with the reproduced signals. The pulses having a voltage higher than the set voltage for comparison were taken out, and their numbers were counted by means of a digital counter (Tōa Denpa Sha). The cumulative distribution of the voltage levels of the pulses was then sought. Then this was converted into the particle size distribution by means of equation (12). There is a crest analyzer on sale on the market as a pulse height discriminator. However, since it is costly and difficult to obtain, we recently produced a comparator circuit using IC elements which are obtainable inexpensively. Its circuit diagram and its operating characteristics [6] are shown in Figs. 8-a and 8-b for the reader's reference.

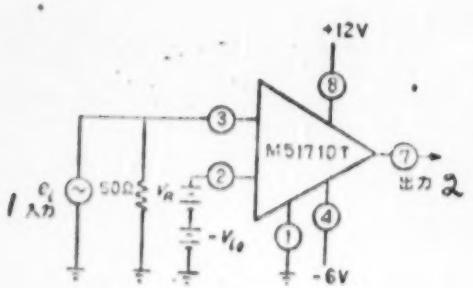

Fig. 8-a. Comparator circuit diagram

Key: 1. Input
2. Output

e_i : Input
V_R : Setting voltage for comparison
V_{10} : Offset

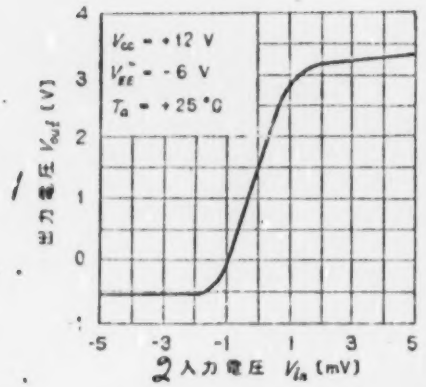

Fig. 8-b. Input-output characteristic curve of M51710 T.

(V_{CC}, V_{EE} : Source voltage)

Key: 1. Output voltage
2. Input voltage

3. Study of Errors Caused by Pulse Overlapping

Since this measuring method is one which utilizes the changes in the luminous flux when particles pass one by one through the slit in the measuring unit, measurement errors will occur if two or more particles are present at the same time in the slit. The method of estimating the probability of the presence of these excessive particles is as described in the following.

The particles passing through the measuring unit will each go through the slit independently of each other and with random intervals. Therefore, the pulses produced here will be random pulses on the time axis. If the number of pulses per unit of time, that is, the mean value of the pulse count, is $\bar{m}$ (number/time), then the probability P that m pulses will

occur in a period of time t will assume a Poisson's distribution as expressed by the following equation:

$$P(m, \bar{m}t) = \frac{\exp(-\bar{m}t)(\bar{m}t)^m}{m!} \tag{13}$$

In the above equation, the probability that m = 0, that is, that there will be no pulses occurring within time t, will be:

$$P(0, \bar{m}t) = \exp(-\bar{m}t) \tag{14}$$

This will also indicate the distribution of the pulse interval t. There will be no possibility at all that the pulses may overlap with each other as long as the slit passage time of the particles is maintained, that is, as long as the particles each maintain an interval equivalent to the pulse width. If the velocity with which the particles pass through the slit part is v and the slit width is H, since the slit passage time is T = H/v, the probability of overlapping of pulses will be:

$$P_E = \int_0^T \bar{m} \exp(-\bar{m}t)\,dt = 1 - \exp(-\bar{m}T) \tag{15}$$

The graph in Fig. 9 plots $\bar{m}$ and T from equation (15) on the x axis and y axis, using P_E as the parameter. In this figure, in order to suppress the probability of pulse overlapping to a value less than P_E^*, it will be sufficient, when the slit passage time of the particles is T*, to adopt a mean number of particles passing through the slit of $\bar{m}^*$ or less. We used glass particles with a mean diameter of about 1.589 mm and took readings of the numbers of pulses within units of time from the electromagnetic oscillogram in order to seek their distribution. Using $\bar{m}$, the mean

number of particles passing through the slit per unit of time, we compared the results with the Poisson's distribution sought from equation (13). The results of this comparison are shown in Fig. 10. Both sets of results agree more or less, and it is clear that the process by which the particles pass through the slit has random characteristics. However, it must be noted that these random characteristics will not apply to powders having adhesive properties or to cases when there is interference between the particles and it is difficult for the particles to become separated from each other.

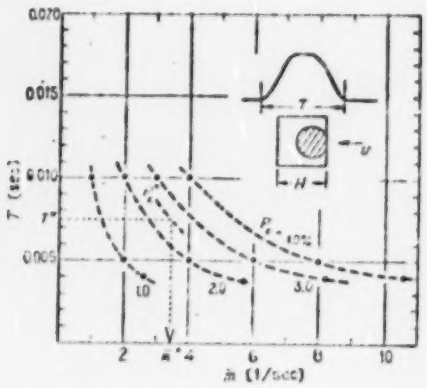

Fig. 9. Calculation of probability of particle overlapping

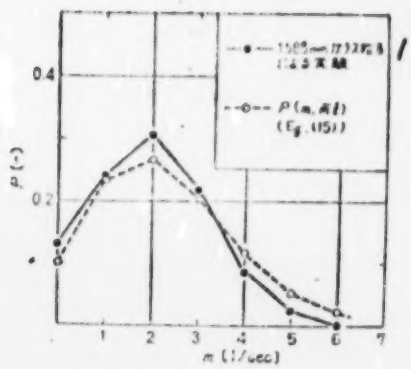

Fig. 10. Comparison of distribution of m and Poisson's distribution

Key: 1. Experiment using 1.589 mm glass particles

4. Test Results, Results of Measurements of Particle Size Distribution, and Discussion

4.1. Tests Using Particles with Uniform Diameters

JIS standard steel balls with diameters of 0.6 and 1.0 mm, opaque glass particles of 1.589 mm, and transparent glass particles with mean diameters of 0.147, 0.209, and 0.346 mm were each used. Approximately 100 particles of each type were used, and the distribution of the $\sqrt{\Delta V/V_0}$ was sought by the electromagnetic oscillograph method. Their mean values and the particle sizes were plotted, and the results are shown in Figs. 11 and 12. It is clear that in every case the square root of the output variation $\Delta V/V_0$ is proportional to the particle diameter d_p. Consequently, C in equation (12) will be a constant regardless of the particle diameter. In slit I and II the values of C were 2.18 mm and 0.581 mm, respectively. Since the light receiver in this equipment was given a rectangular shape, C in equation (12) will be $2H\sqrt{\pi k}$ (it was

assumed that the slit width and the width of the light receiver were both the same). When k was calculated after substituting the experimental values for C, the values were found to be k = 1.07 and 0.943 for slit I and slit II, respectively, and it was ascertained that $k \approx 1$. Since the slits were made by hand, it was thought that there might have been some errors in their dimensions. When the cumulative distribution was sought for particles having approximately uniform diameters, results such as those shown in Fig. 13 were obtained.

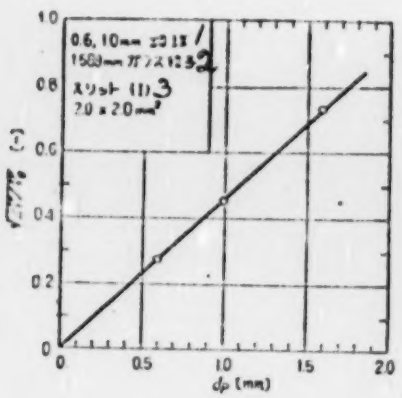

Fig. 11. Relationship between d_p and $\sqrt{\Delta V/V_0}$ (C = 2.18 mm)

Key: 1. Steel balls of 0.6 and 1.0 mm
2. Glass particles of 1.589 mm
3. Slit (I)

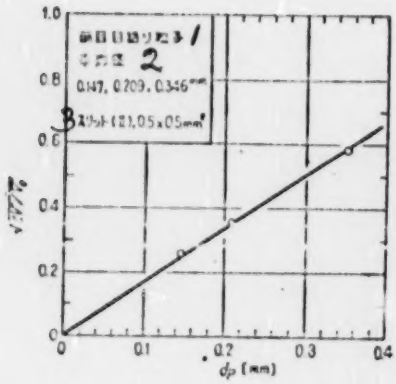

Fig. 12. Relationship between d_p and $\sqrt{\Delta V/V_0}$ (C = 0.581 mm)

Key: 1. Particles clogging sieve apertures
2. Mean diameter
3. Slit (II)

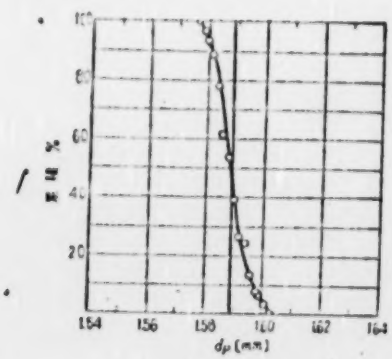

Fig. 13. Results of measurement of cumulative distribution of glass particles (precision 13/1000) having approximately uniform diameters (mean diameter 1.589 mm)

Key: 1. Cumulative distribution

4.2. Results of Measurements of Particle Size Distribution

In Figs. 14 and 15 are shown the results of measurements of the particle size distributions for two sets of 100 glass particle samples (a) and (b), each of them having different particle size distributions. The particle size distributions were measured by means of micrometers. The data recorder-comparator method and the electromagnetic oscillograph method were used, with slit I, and the particle supply speed was suppressed so as to minimize errors caused by overlapping pulses as explained in section 3. The results of measurements obtained by these methods differed somewhat from the results of micrometer measurements within the range of the smaller particle sizes, but one may say in general terms that there was a good agreement.

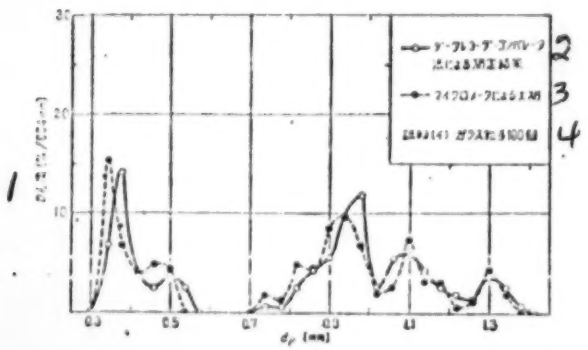

Fig. 14. Results of measurements of particle size distribution by the data recorder-comparator method

Key:
1. Frequency
2. Results of measurements by the data recorder-comparator method
3. Measurements by micrometer
4. Samples (a): 100 glass particles

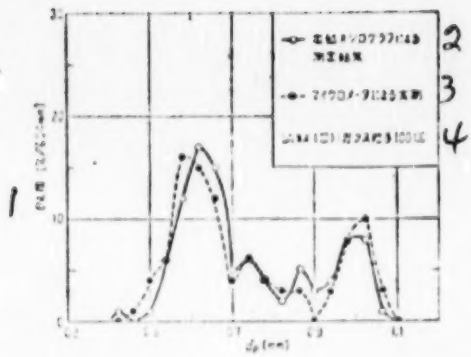

Fig. 15. Results of measurements of particle size distribution by the electromagnetic oscillograph method

Key:
1. Frequency
2. Results of measurements by the electromagnetic oscillograph method
3. Measurements by micrometer
4. Samples (b): 100 glass particles

The lower limit of the particle size which can be measured with a single slit is determined by the noise contained in the signals. For example, when the data recorder-comparator method is used, the noise will be determined by the S/N ratio of the data recorder. In the cases described in this report, the S/N ratio was 43 dB. Therefore, in slit I, it will theoretically be possible to make measurements up to about 230 microns. However, in the experiments, the lower limit of the measurements was about 300 microns. Consequently, slit II was used in the measurements of particles of less than 300 microns.

5. Concerning the Measuring Time and Sample Quantities

When the number of particles and the speed with which the particles are supplied into the measuring instrument are determined so as to minimize the sample error and errors caused by pulse overlapping, the measuring time for one sample is determined accordingly. For example, if 1,000 particles are supplied so that they will pass through the slit at a speed of 1,000 mm/sec, if the slit width is 2.0 mm, T will be 0.002 sec. If it is desired to suppress the probability of overlapping to 3.0%, it will be sufficient, on the basis of equation (15), to have a mean supply speed $\bar{m}$ of less than 15 particles per second. Therefore, the measuring time will be 1,000/15 66 sec. or more. If we suppose that the particle sizes are divided up into 10 size intervals, it will be possible to seek the distribution of the particle size numbers by taking direct readings from the digital counter in about 10 minutes, if we exclude the time for rewinding the data recorder and the time for switching the comparative voltages in the comparator. The signal processing time will be reduced to one-eighth if the tape speed is changed over, for example, to four times the speed after the signals have been recorded on the data recorder, and if a two-channel digital counter is also used.

In this case, the necessary weight of the particle samples will be very small. For instance, if one uses glass particles with a mean diameter of 0.8 mm, the necessary weight will be about 0.7 g.

Conclusion

An optical measurement device for particle size distributions was developed consisting of a combination of a parallel light ray source and a light receiver made of optical fiber bunches. The amount of light intercepted by each individual particle is observed in order to seek the particle size distribution. As a result, the following findings were obtained.

(1) It was ascertained that the following relationship applies between the diameter of the individual particles and the output voltage of the photomultiplier:

$$d_p = C\sqrt{\Delta V / V_0} \tag{12}$$

(2) When using equation (12) to measure the particle size distribution, in order to suppress errors caused by overlapping of particles, it is possible to use the following to estimate the probability of overlapping:

$$P_x = 1 - \exp(-\bar{n}T) \tag{15}$$

(3) The time required for finding the particle size distribution can be shortened by relying on an analog method of processing the signals using the data recorder-comparator method.

(4) Only a small amount of samples is necessary for measuring the particle size distribution.

(5) The results of measurements of the particle size distributions coincided well with the counts obtained by actual measurements.

Nomenclature

A_R	: Area of slit or light receiver	[mm^2]
F	: Luminous flux	[lm]
F_0	: Luminous flux passing through slit	[lm]
ΔF	: Decrease of luminous flux when particles are present	[lm]
H	: Slit width	[mm]
I	: Total luminous flux entering light receiver	[lm]
i	: Number of reflections	
j	: Coordinate index	
k	: Ratio of luminous flux which does not reach the light receiver after being admitted to the particle surface (equation (1))	[-]
L	: Radius of light receiver	[mm]
l_x	: Distance shown in Fig. 2	[mm]
m	: Number of particles passing through slit during time t, or number of pulses	[-]
$\bar{m}$	: Mean number of particles passing through slit per unit time	[1/sec]
N	: Number of parallel light beams admitted to particles for purpose of calculating k	
n	: Refractive index	
$P(m, \bar{m}t)$	: Poisson's distribution expressed in equation (12)	[-]
P_E	: Probability of overlapping of particles in slit	[-]
R	: Radius of particle (= $d_p/2$)	[mm]
rj	: = $\Delta r/2 + \Delta r(j-1)$	[mm]

Δr :	$= R/N$	[mm]
S :	Distance between center of particle and light receiver	[mm]
T :	$= H/v$, time to pass through slit	[sec]
t :	Time	[sec]
U_i :	Angle defined in Fig. 3	[rad]
V_i :	Angle defined in Fig. 3	[rad]
V_0 :	Output of photomultiplier at $F = F_0$	[V]
ΔV :	Reduction of output voltage corresponding to ΔF	[V]
v :	Velocity of particles passing through slit	[mm/sec]
$\Delta\theta$:	Microangle shown in Fig. 2	[rad]
μ :	Reflectance (equation (9))	[-]

Bibliography

1. Matsumoto, Kanji and Mori, Yoshiro: Kagaku kōgaku, 36, 1137 (1972).
2. Jimbo, Genji et al.: Preprint, 4th Autumn Convention, Japanese Society of Chemical Engineers, F-201, Hiroshima (1970).
3. Kubota, Hiroshi: Kōgaku [Optics], Iwanami Shoten, 1971, p. 306.
4. Denki Gakkai [Institute of Electrical Engineers of Japan]: Shōmei kōgaku [Illumination engineering], 1960, p. 176.
5. Hamamatsu Terebi Kabushiki Kaisha: Kōden henkan soshi shiryō [Catalog of photoelectric tubes], 1971.
6. Mitsubishi Electric Corporation: Handōtai shūseki kairo sokuhō [Bulletin on semiconductor integrated circuits], 1970.